Vol. 11, No. 3, 2025

Volodymyr Maistruk¹, Pavlo Maistruk²

- ¹ Department of Designing Machine and Automotive Engineering, Lviv Polytechnic National University, 12, S. Bandery str., Lviv, Ukraine, E-mail: volodymyr.v.maistruk@lpnu.ua, ORCID 0000-0001-6982-8592
- ² Department of Robotics and Integrated Mechanical Engineering Technologies, Lviv Polytechnic National University, 12, S. Bandery str., Lviv, Ukraine, E-mail: pmaystruk@gmail.com, ORCID 0000-0003-0662-1935

RESEARCH ON THE MAIN CHARACTERISTICS OF SPIRAL DIRECT-FLOW CYCLONES WITH A FLAT COVER

Received: August 29, 2025 / Revised: September 16, 2025 / Accepted: October 06, 2025

© Maistruk V., Maistruk P., 2025

https://doi.org/10.23939/ujmems2025.03.069

Abstract. An analysis of works in which the designs of dust collection devices, which are often used in industry, are studied using CFD programs has been conducted. It has been established that numerical modeling and simulation methods for predicting the operation of dust collection devices under specific conditions are most effective, as they are widely used in research on devices of this type. Using numerical modeling methods, the radial distribution of pressure, velocity, and the tangential, radial, and axial components of the gas flow velocity in a spiral direct-flow cyclone has been studied for cases of operation on both the discharge and suction lines. A comparative analysis of the tangential component of the velocity has been conducted, revealing that the key characteristics of the tangential velocity, which underpin particle separation, are preserved in both operating modes. Differences in the absolute values of the tangential component of the velocity, as well as its influence on the intensity of the vortex motion, have been identified. For the radial component of the velocity, the comparative analysis revealed that the main regularities of radial flow formation, which are critical for particle deposition on the walls, are preserved in both operating modes. Differences in the absolute values of the radial component of velocity were found for different modes, which may affect efficiency. For the axial component of the velocity, the comparative analysis showed the presence of downward and upward flows characteristic of cyclones, with the main regularities preserved in both operating modes. Differences in the absolute values of the axial component of the velocity and the intensity of the reverse flows were found. The aerodynamic resistance of the device under study was determined. It was established that at a speed in the inlet pipe of ~15 m/s, the difference in aerodynamic resistance between the operating mode on the suction line and the discharge line is about 15 Pa. With an increase in the speed to a value of ~23.5 m/s, this difference increases to more than 50 Pa. The total and fractional efficiencies of the cyclone were determined for different operating modes of the apparatus and gas flow rates. It was established that to achieve maximum efficiency of gas purification, this spiral direct-flow cyclone should be operated on the suction line and at optimal velocities in the inlet pipe of 21–24 m/s. It was determined that for particles with a size of 3–8 μm, the difference in fractional efficiency between the case when particles are considered captured if they reach the wall of the cylindrical part of the apparatus body and the case when particles are considered captured if they reach the wall of the conical part of the body is the most noticeable.

Keywords: CFD modeling, degree of purification, hydraulic resistance, energy efficiency, tangential, radial, axial components of velocity.

Introduction

Cyclones are one of the most common and cost-effective devices for removing solid particles from gas flows in various industrial sectors, including cement, metallurgical, chemical, and energy. The efficiency of dust collection in cyclones largely depends on their geometry, gas and particle properties, as well as on

the operating mode. Traditional methods of cyclone design and optimization, based on empirical models and experimental studies, are often laborious and expensive. With the advent and development of computational fluid dynamics (CFD), it has become possible to study complex flow phenomena inside cyclones in detail, predict their efficiency, and optimize design without the need for expensive full-scale experiments.

Problem Statement

To solve practical problems of improving cyclone dust collection devices, theoretical methods are of great importance; the use of which, using mathematical modeling, numerical methods, and modern computer technology, allows you to quickly and with high probability determine process parameters, such as the movement of dust particles in a gas stream. Knowledge of the structure of the gas stream, in particular the distribution of tangential, radial and axial velocity components along the radius of the device, aerodynamic resistance, and the efficiency of dust particle capture will allow you to evaluate the effectiveness of the studied dust collector design in a multifaceted way.

Review of Modern Information Sources on the Subject of the Paper

CFD modeling of cyclones has become an integral part of engineering practice and scientific development. Early work focused on verifying CFD models by comparing them with experimental data, whereas modern research encompasses a broader range of issues, including geometry optimization, studying the effects of various operating parameters, developing new structures, and analyzing wear.

One of the key aspects of CFD modeling of cyclones is selecting the appropriate turbulence model. Most studies employ RANS (Reynolds Averaged Navier-Stokes) models, particularly the k- ϵ and k- ω models. For example, study [1] demonstrates the effectiveness of using the k- ϵ turbulence model to predict pressure drop and particle capture efficiency in cyclones. The authors emphasize the importance of selecting the appropriate boundary conditions for obtaining accurate results. Similar conclusions were drawn in [2], where the k- ϵ model also demonstrated a good correlation with experimental data when modeling the flow inside standard cyclones.

However, some researchers point out the limitations of standard RANS models, particularly when modeling highly turbulent flows and secondary flows that occur in cyclones. In such cases, more sophisticated models such as RSM (Reynolds Stress Model) or LES (Large Eddy Simulation) can be used. The work [3] compares the effectiveness of various turbulence models, including RSM and LES, in modeling multiphase flow within a cyclone. The authors show that RSM and LES can provide more accurate predictions, especially for small particles, but require significantly more computational resources. This is confirmed in the study [4], where LES modeling was successfully applied to a detailed analysis of turbulent structures and their influence on particle trajectories in a cyclone. A key direction is the optimization of cyclone geometry to enhance dust collection efficiency and minimize pressure drop. The study [5] uses CFD to optimize the inlet angle and outlet diameter, demonstrating a significant improvement in cyclone performance. Similarly, in [6], a parametric analysis was conducted to investigate the effect of various geometric parameters, including cyclone diameter, cone height, and inlet and outlet dimensions, on cyclone aerodynamics and efficiency. The results showed that small changes in geometry can significantly affect dust collection efficiency.

Many studies have focused on multiphase modeling, which enables the tracking of particle trajectories and the prediction of capture efficiency. The Discrete Phase Model (DPM) is a widely used approach to track the motion of individual particles in a gas flow. In [7], DPM was applied to study the behavior of particles of different sizes in a cyclone, enabling the visualization of particle accumulation zones and the prediction of fractional capture efficiency. The authors also consider the effects of drag, lift, and Brownian motion on the trajectories of particles. The study [8] further develops this approach, including particle-particle interactions, which are important for modeling highly concentrated flows.

In addition to traditional cyclones, CFD is also used to study and optimize new and modified designs. Work [9] examines the efficiency of multicyclones and the impact of inlet and outlet configurations on their performance. The use of CFD allowed the identification of high-velocity zones and potential clogging problems. Study [10] is devoted to the study of axial-inlet cyclones, which can be more compact and efficient for certain applications. CFD modeling helped to optimize the swirler parameters and calculate the optimal conditions for maximum particle capture.

An important aspect is also the energy efficiency of cyclones, which is closely related to the pressure drop. CFD enables the evaluation of pressure drop and the identification of areas with high energy losses. In a study [11], the cyclone geometry was optimized to minimize the pressure drop while maintaining a significant reduction in dust collection efficiency. The results of CFD modeling were used to identify recirculation zones and eddy currents that cause energy losses.

Some publications focus on the influence of particle properties on cyclone efficiency. Work [12] investigates the influence of particle shape (spherical, non-spherical) and density on the trajectories and capture efficiency using CFD. The authors emphasize that ignoring the non-sphericality of particles can lead to significant prediction errors. This is an important aspect for modeling real industrial processes, where particles often have irregular shapes.

With the development of computing power, there are more and more works using hybrid approaches that combine CFD with other optimization algorithms, such as genetic algorithms or Monte Carlo methods. Study [13] applies a combination of CFD and a genetic algorithm for the multi-criteria optimization of cyclones, aiming to simultaneously maximize capture efficiency and minimize pressure drop.

A future direction of research is the application of CFD to model complex physical phenomena occurring in cyclones, such as particle agglomeration, cyclone wall wear, and the influence of electrostatic forces. Work [14] explores the potential application of CFD in predicting cyclone wear caused by abrasive particles. The authors model particle collisions with walls and estimate the erosion rate. This allows designing cyclones with increased wear resistance. Finally, study [15] demonstrates the potential of using CFD to model electrostatic cyclones, where electrostatic fields are employed to enhance the efficiency of capturing small particles.

The purpose and objectives of the study

Knowledge of the structure of the gas flow, particularly the pressure distribution, as well as the tangential, radial, and axial components of the absolute velocity along the radius of the device, will enable us to determine the hydraulic resistance, fractional, and total dust capture efficiency. This will allow us to assess the efficiency of the spiral direct-flow cyclone. It is advisable to conduct research using numerical modeling and simulation methods for the separation process (e.g., CFD programs).

Objectives and Problems of Research

Numerical calculations of aerodynamic characteristics of the flow in spiral direct-flow cyclones. The integration of advanced computer technologies has become an integral part of modern scientific activity, enabling the accurate calculation of key equipment parameters during its development stage. For the effective design of innovative dust collectors, computer reproduction of their aerodynamic properties is a critically important tool.

One effective method for mathematically describing the physics of separating solid impurities from gas flows is the use of computer-aided design and engineering analysis platforms, known as CAD/CAE systems.

Of particular value in this context are software complexes that can integrate with geometric CAD. Such a combination provides powerful tools for a deep and comprehensive analysis of complex aerodynamic and thermophysical phenomena.

To simulate the flow, a physical model of fluid motion was used - the Navier-Stokes equation, which in general vector form has the form [16]:

$$\frac{d\bar{\vartheta}}{dt} = \bar{F} - \frac{1}{\rho} gradP + v\Delta\bar{\vartheta} , \qquad (1)$$

where $\bar{\vartheta}$ – air speed vector; \bar{F} – mass force vector; ρ – air density; P – air pressure at any point; v – kinematic viscosity of air.

The Navier-Stokes equations system in its non-stationary form mathematically formulates the fundamental principles of conservation of mass, momentum and energy for a moving medium. This mathematical apparatus is universal and allows for the reproduction of various modes of motion of a liquid or gas, in particular, laminar, turbulent, and transient.

When analyzing turbulent flows, a special procedure is used - averaging of the Navier-Stokes equations by Reynolds (RANS). This approach enables the consideration of the impact of small-scale turbulent pulsations on the average flow characteristics. At the same time, to describe macroscopic changes in averaged gas-dynamic quantities (pressure, velocity, temperature), the corresponding time derivatives are added to the equations.

The consequence of the averaging procedure is the appearance in the equations of new terms, known as Reynolds stresses. To ensure the mathematical closure of the resulting system, it is supplemented with a turbulence model. One of the most common is the k- ε model, which introduces two additional equations for the transport of the kinetic energy of turbulence (k) and the rate of its dissipation (ε) .

Thus, the final system of equations describing the conservation laws for an unsteady three-dimensional flow is formulated within the framework of the Euler approach. It is written in a Cartesian coordinate system $(x_i, \text{ where } i = 1, 2, 3), \text{ which, in turn, rotates with angular velocity } \Omega$ about an axis passing through its center:

$$\frac{\partial p}{\partial t} + \frac{\partial}{\partial x_k} (\rho u_k) = 0, \tag{2}$$

$$\frac{\partial p}{\partial t} + \frac{\partial}{\partial x_k} (\rho u_k) = 0,$$

$$\frac{\partial (\rho u_i)}{\partial t} + \frac{\partial}{\partial x_k} (\rho u_i u_k - \tau_{ik}) + \frac{\partial P}{\partial x_i} = S,$$
(2)

$$\frac{\partial(\rho E)}{\partial t} + \frac{\partial}{\partial x_k} ((\rho E + P)u_k + q_k - \tau_{ik} u_i) = S_k u_k + Q_H, \tag{4}$$

where t – time; u – fluid velocity; ρ – fluid density; P – fluid pressure;

$$S_i = S_{iporous} + S_{igravity} + S_{irotation} , (5)$$

Where S_i – external mass forces acting on a unit mass of fluid: $S_{iporous}$ – influence of the resistance of a porous body, $S_{igravity}$ – influence of gravity, $S_{iroration}$ – the effect of rotation of the coordinate system, i.e.

The kinetic energy of turbulence k and the dissipation of this energy ε are determined by solving the following two equations:

$$\frac{\partial pk}{\partial t} + \frac{\partial}{\partial x_k} (\rho u_k k) = \frac{\partial}{\partial x_k} \left[\left(\mu_i + \frac{\mu_i}{\sigma_k} \right) \frac{\partial k}{\partial x_k} \right] + S_k \quad , \tag{6}$$

$$\frac{\partial p\varepsilon}{\partial t} + \frac{\partial}{\partial x_k} (\rho u_k \varepsilon) = \frac{\partial}{\partial x_k} \left[\left(\mu_i + \frac{\mu_i}{\sigma_{\varepsilon}} \right) \frac{\partial k}{\partial x_k} \right] + S_{\varepsilon} , \qquad (7)$$

where

$$S_k = \tau_{ij}^R \frac{\partial u_i}{\partial x_i} - \rho \varepsilon + \mu_i P_B , \qquad (8)$$

$$S_{\varepsilon} = C_{\varepsilon 1} \frac{\varepsilon}{k} \left(f_i \tau_{ij}^R \frac{\partial u_i}{\partial x_j} + \mu_i C_B P_B \right) - C_{\varepsilon 2} f_2 \frac{\rho \varepsilon^2}{k} \quad , \tag{9}$$

$$\tau_{ij}^{R} = \mu_{i} \left(\frac{\partial u_{i}}{\partial x_{j}} + \frac{\partial u_{j}}{\partial x_{i}} - \frac{2\partial u_{i}}{3\partial x_{i}} \sigma_{ij} \right) - \frac{2}{3} \rho k \delta_{ij} ; P_{B} = -\frac{g_{i}}{\sigma_{B}} \frac{1}{\rho} \frac{\partial p}{\partial x_{i}} , \qquad (10)$$

where g_i – component of gravitational acceleration in the coordinate direction x_i , $\sigma_B = 0.9$ and $C_B = 1$ at $P_{\rm B} > 0$ and $C_{\rm B} = 0$ at $P_{\rm B} \le 0$, $C_{\epsilon 1} = 1.44$, $C_{\epsilon 2} = 1.92$, $\sigma_k = 1.0$, $\sigma_{\epsilon} = 1.3$.

The influence of gravity forces is modeled using the Sigravity component, which is included in the total mass force (5) in equations (6, 7):

$$S_{igravity} = -\rho g_i \,, \tag{11}$$

where g_i – the i-th component (along the i-th axis of the coordinate system) of the gravitational acceleration vector.

The process of obtaining a numerical solution involves transforming a continuous and non-stationary mathematical model of physical phenomena into a discrete format, taking into account spatial and temporal parameters.

To implement spatial discretization, the entire computational zone of the apparatus, which includes the fluid and solid fractions, was divided into finite volumes using a computational grid. The faces of its elements were oriented parallel to the coordinate planes XY, XZ and ZY.

When analyzing the dynamics of the fluid within the closed geometry of the model, the method of fictitious regions was used. Its essence lies in the fact that the computational grid is generated for a conditional region in the form of a parallelepiped, which completely covers the object under study. However, direct calculations were carried out exclusively for those cells that were physically located within the space filled with the flow, according to the problem's conditions.

Since the standard faces of the mesh elements could not accurately reproduce the curved surfaces of solids in contact with the environment, local cell refinement was introduced in areas of the device with complex geometry. Ultimately, the generated computational mesh consisted of 2.032.539 elements.

The object under study. In this work, a spiral direct-flow cyclone was investigated. The structure and principle of operation of this cyclone are presented in [17, 18]. The spiral direct-flow cyclone consists of a vertically placed housing, the upper cylindrical part 1, which in cross-section has the form of an Archimedean spiral, closed on top by a cover 2 to which a stabilizer 4 is fixed by means of a flange 3, the bottom 5 of which is made in the shape of a cone, a coaxial insert 6, a tangential inlet pipe 7, installed at an angle relative to the generating upper part of the housing 1, pipes 8 and 9 for removing deposited dust and purified gas flow, respectively, and a connecting flange 10, which connects the upper cylindrical 1 and lower conical 11 parts of the housing.

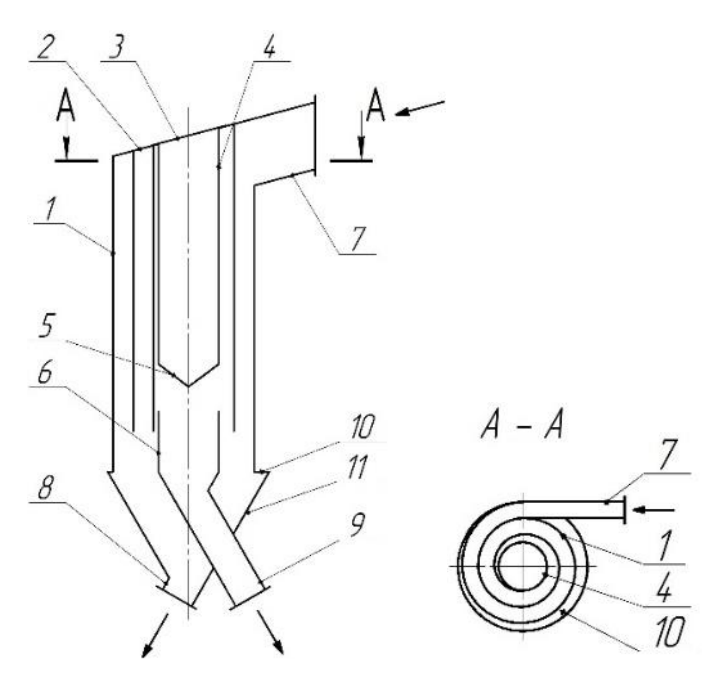


Fig. 1. Schematic diagram of a spiral direct-flow cyclone

The spiral direct-flow cyclone operates as follows. The dusty gas enters through the tangential inlet 7 into the spiral channel of the annular space of the upper cylindrical part of the housing 1 and is twisted. Under the action of centrifugal forces that arise during the rotation of the flow, parts of the dust are thrown to the periphery, move down along the wall of the upper cylindrical part of the housing 1, then through the annular gap between the lower conical part of the housing 11 and the coaxial insert 6, and are discharged through the dust discharge pipe 8. The purified gas enters the space of the coaxial insert 6 and is discharged through the purified gas discharge pipe 9.

The study of the operation of the above-described spiral direct-flow cyclone design was conducted using numerical methods and CFD programs. For this purpose, a 3D model of the device was created in the CAM program, with the dimensions of the inlet pipe matching those of a standard cyclone with a diameter of 150 mm. The initial parameters for studying the created 3D model of the device were the characteristics of the dust-air flow: atmospheric pressure under normal conditions $P_0 = 101325$ Pa; ambient temperature under normal conditions $T_0 = 293$ K; air density $\rho_{pov} = 1.293$ kg/m³; dust – quartz dust, density $\rho_{py} = 600 \text{ kg/m}^3$; dust fractional composition: 0–1 μ m – 5 %; 1–3 μ m – 14 %; 3–5 μ m – 16 %; 5– 6 μ m – 5.5 %; $6-8 \mu m - 9.5 \%$; $8-10 \mu m - 8 \%$; $10-12 \mu m - 4 \%$; more than $12 \mu m - 38 \%$. The fractional composition of the dust corresponded to the composition of the KP-3 dust, for which the median particle diameter is 8 microns, and which is used as a standard for comparative tests of inertial-type dust collectors. The following boundary conditions were set for the calculation: open flow - volume flow rate (0.044156 m³/s; 0.052987 m³/s; 0.061819 m³/s; 0.07065 m³/s); open pressure – ambient pressure; wall – real wall. The values of the volume flow rates corresponded to the following velocities in the inlet pipe: 14.719 m/s, 17.662 m/s, 20.606 m/s, and 23.55 m/s. For a standard cyclone with a diameter of 150 mm, the velocity data in the inlet pipe correspond to fictitious velocities of 2.5 m/s, 3 m/s, 3.5 m/s, and 4 m/s, respectively.

To simulate the process when the device operates on the discharge line, the boundary conditions at the inlet to the device were set as follows: open flow – volumetric flow rate at the inlet Q_{in} m³/s, and at the outlet: open pressure – ambient pressure P_{out} , Pa. If the device operates on the suction line, then the open pressure at the inlet is set as follows: ambient pressure P_{in} , Pa, and at the outlet from the device: open flow – volumetric flow rate at the outlet Q_{out} m³/s.

The aerodynamic resistance was determined by the difference in pressures at the inlet and outlet of the device. When determining cleaning efficiency, it was assumed that all dust particles are spherical in shape and do not interact with each other. The cleaning efficiency was determined for two cases. In the first case, when determining the cleaning efficiency, it was assumed that particles were considered captured when they reached the wall of the upper cylindrical part of the apparatus body, i.e., they could not be carried away again by the gas flow (representing the maximum possible cleaning efficiency). In the second case, it was assumed that the particles were considered captured when they reached the wall of the lower conical part of the apparatus body (minimum possible cleaning efficiency).

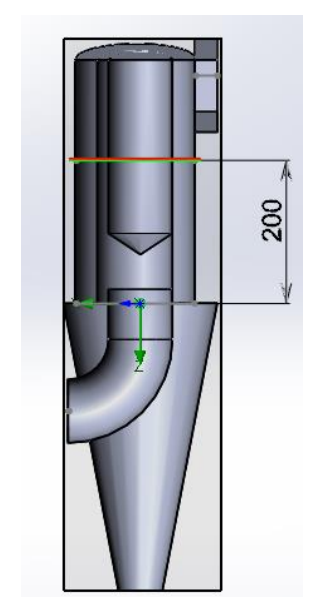


Fig. 2. Schematic representation of the location of the research plane

Main Material Presentation

The parameters analyzed in this work were the change in pressure, velocity, tangential, radial, and axial velocity components along the radius and height of the device, as well as aerodynamic resistance and total and fractional cleaning efficiency in the studied cyclone for different operating modes of the device.

The distribution of pressure, velocity, and velocity components in the cyclone was studied in the cylindrical (separation) zone, which is 200 mm above the plane of transition from the cylindrical part to the conical one (Fig. 2). According to the study results, corresponding graphs were constructed.

Comparative analysis of the pressure distribution in a spiral direct-flow cyclone when operating on the discharge and suction lines. The presented radial pressure distribution in the annular space of the upper part of the spiral direct-flow cyclone (Fig. 3, 4) illustrates the contribution of each turn. The range of values on the abscissa axis from 0.0605 to 0.0905 m corresponds to the location of half a turn of the first turn after the inlet pipe, the region from -0.075 to -0.045 m corresponds to the full turn of the first turn, the region from 0.045 to 0.0605 m corresponds to the location of half a turn of the second turn.

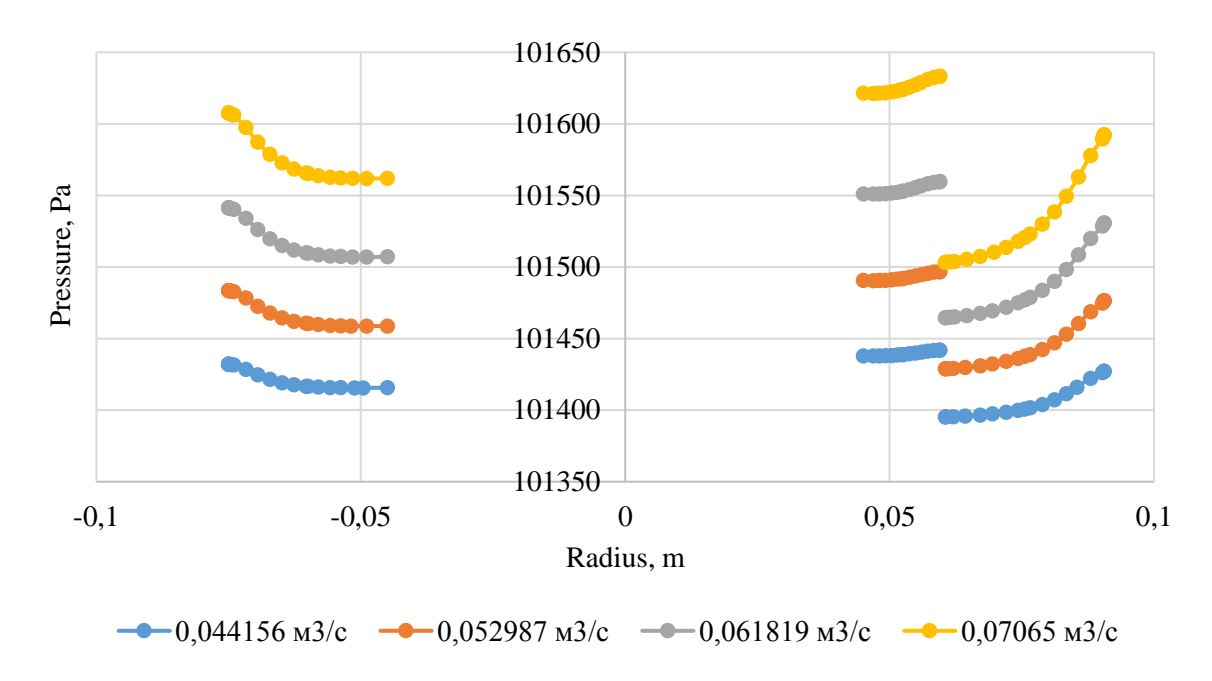


Fig. 3. Total pressure distribution in the cross section of a spiral direct-flow cyclone operating on the discharge line

For all flows (Fig. 3), a clear pattern is observed: the pressure decreases as the radius increases. This is a characteristic feature of vortex motion: in the center of the vortex, the pressure is lowest, while on the periphery, it is highest. This is due to centrifugal forces that cause the gas to move to the periphery, creating a rarefaction in the central part. At higher flows, the pressure difference between the center and the periphery becomes more pronounced, which indicates an intensification of vortex motion.

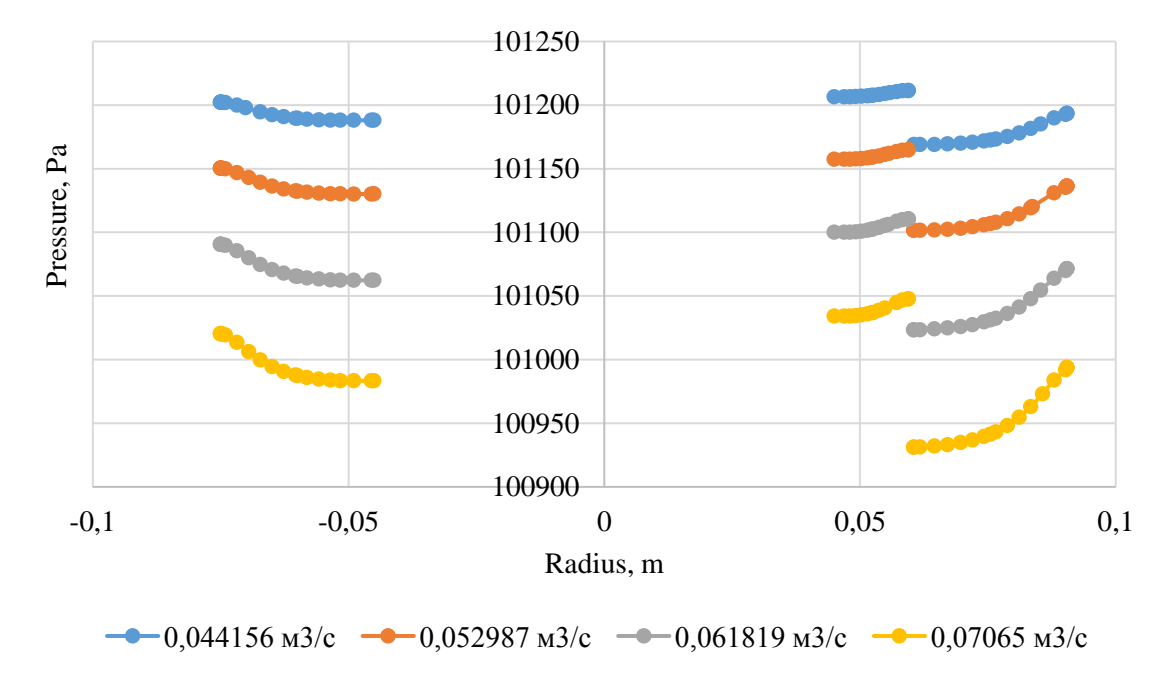


Fig. 4. Total pressure distribution in the cross section of a spiral direct-flow cyclone operating on the suction line

In Fig. 4, all curves show a pressure that is lower than atmospheric (approximately 101325 Pa). This is expected, since the cyclone operates before the fan, which creates a vacuum in the system.

As in the case of the discharge operation, a decrease in pressure is observed as the radius increases. However, unlike Fig. 3, where the pressure at small radii was the lowest and gradually increased towards the

periphery, here we see that the pressure approaches the atmospheric value at large radii and drops significantly as it approaches the center. This indicates that the greatest vacuum is formed in the central part of the cyclone, where the vortex flow is formed. Also, as in Fig. 3, at higher flows, the pressure difference between the center and the periphery becomes more pronounced, confirming the strengthening of the vortex effect.

Comparative analysis of the velocity distribution. The efficiency of cyclones depends largely on the internal aerodynamics, in particular on the velocity distribution in the working volume. Straight-flow cyclones are characterized by lower aerodynamic resistance compared to traditional cyclones, which makes them attractive for many industries.

Both graphs (Fig. 5, 6) show the tangential velocity distribution characteristic of vortex devices. The velocity initially increases from the central axis to a certain radius, and then sharply decreases in the near-wall region. This indicates the formation of a vortex core with predominantly solid-state rotation in the central part and a free vortex on the periphery. The peak velocity values correspond to the region of maximum flow swirl, where centrifugal forces are most intense, contributing to the separation of dust particles.

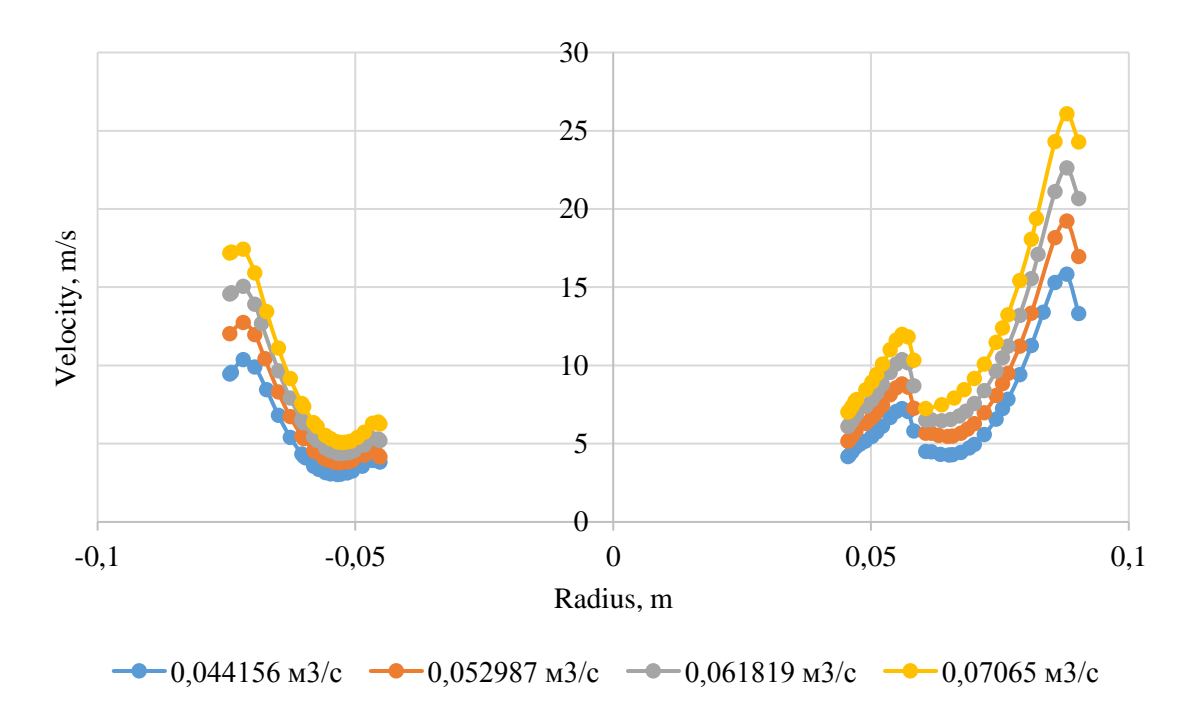


Fig. 5. Velocity distribution in the cross section of a spiral direct-flow cyclone operating on the discharge line

For both operating modes (discharge and suction), the absolute value of the velocity increases with increasing gas flow rate over the entire range of radii. This is expected, as a larger gas volume flow results in higher velocities within the confined volume of the cyclone. The intensity of the vortex motion also increases, which contributes to better dust capture, but may lead to increased aerodynamic drag.

On the discharge line (Fig. 5), the peak velocity values reach approximately 26 m/s at maximum flow rate. On the suction line (Fig. 6), the peak velocity values are somewhat lower, reaching approximately 21 m/s at maximum flow rate. This difference can be explained by the compressibility of the gas. When operating on the discharge line, the gas is under higher pressure, resulting in a higher density. To ensure the same volumetric flow rate, the linear velocity of the gas under pressure can be higher, since the gas flow has greater kinetic energy, which is converted into tangential velocity. On the suction line, where the gas is rarefied, its density is lower, resulting in somewhat lower absolute velocities at the same volumetric flow rate.

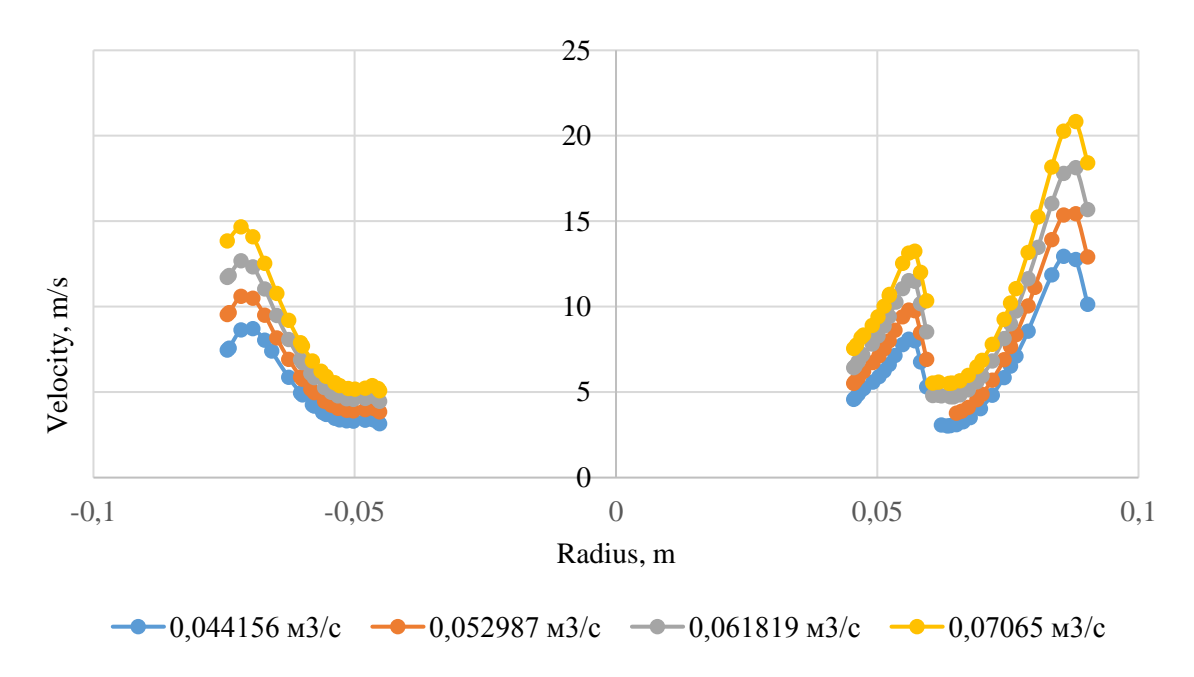


Fig. 6. Velocity distribution in the cross section of a spiral direct-flow cyclone operating on the suction line

The shape of the velocity profile (increasing from the center, reaching a maximum, and then decreasing towards the walls) is similar for both cases. This indicates the universality of the mechanism of vortex flow formation in this type of cyclone.

However, it can be noted that when operating on the discharge line (Fig. 5), the velocity peaks are somewhat more pronounced and sharper, and the velocity drop near the walls is less sharp than on the suction line (Fig. 6). This may be due to the fact that under excess pressure the flow is more "rigid" and less prone to rapid velocity decay in the near-wall region due to interaction with friction against the walls.

Comparative analysis of the distribution of the tangential velocity component. Tangential velocity is a crucial kinematic characteristic of cyclone flow, as it determines the magnitude of the centrifugal force that separates solid particles from the gas flow. Determining tangential velocity is a key task during the design and operation of cyclones to achieve high dust collection efficiency and minimize energy consumption.

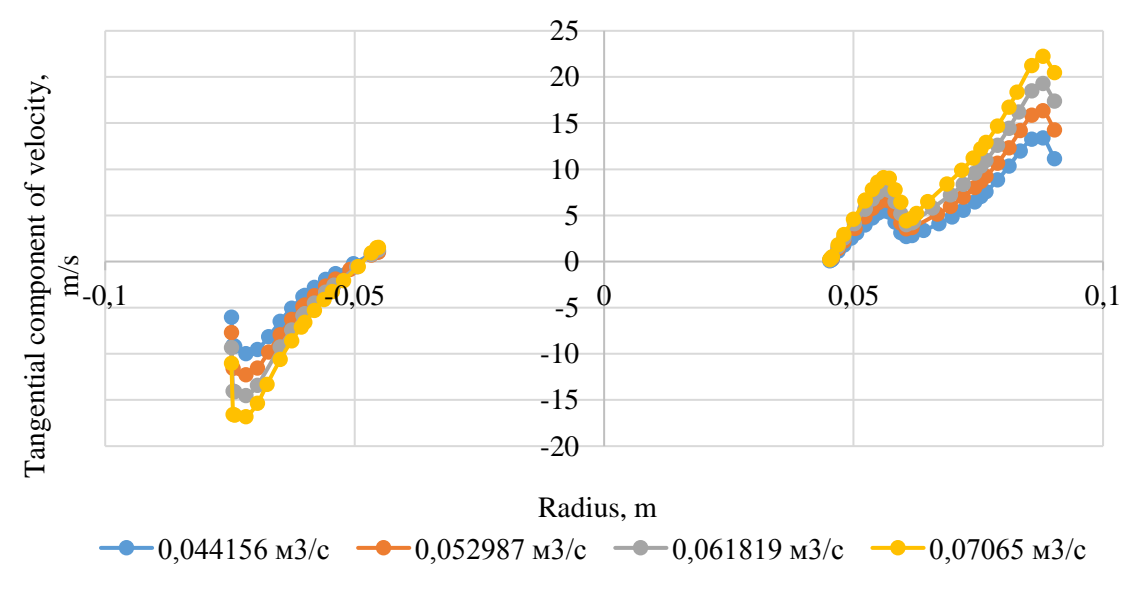


Fig. 7. Distribution of the tangential velocity component in the cross section of a spiral direct-flow cyclone operating on the discharge line

Both graphs (Fig. 7, 8) display a classic tangential velocity distribution characteristic of cyclones. The velocity increases from the central axis to a certain radius, reaching maximum values, and then decreases as it approaches the cyclone walls. The maximum values of the tangential velocity, both positive and negative (reflecting opposite directions of flow rotation in different parts of the cross section), indicate the intensity of the vortex motion.

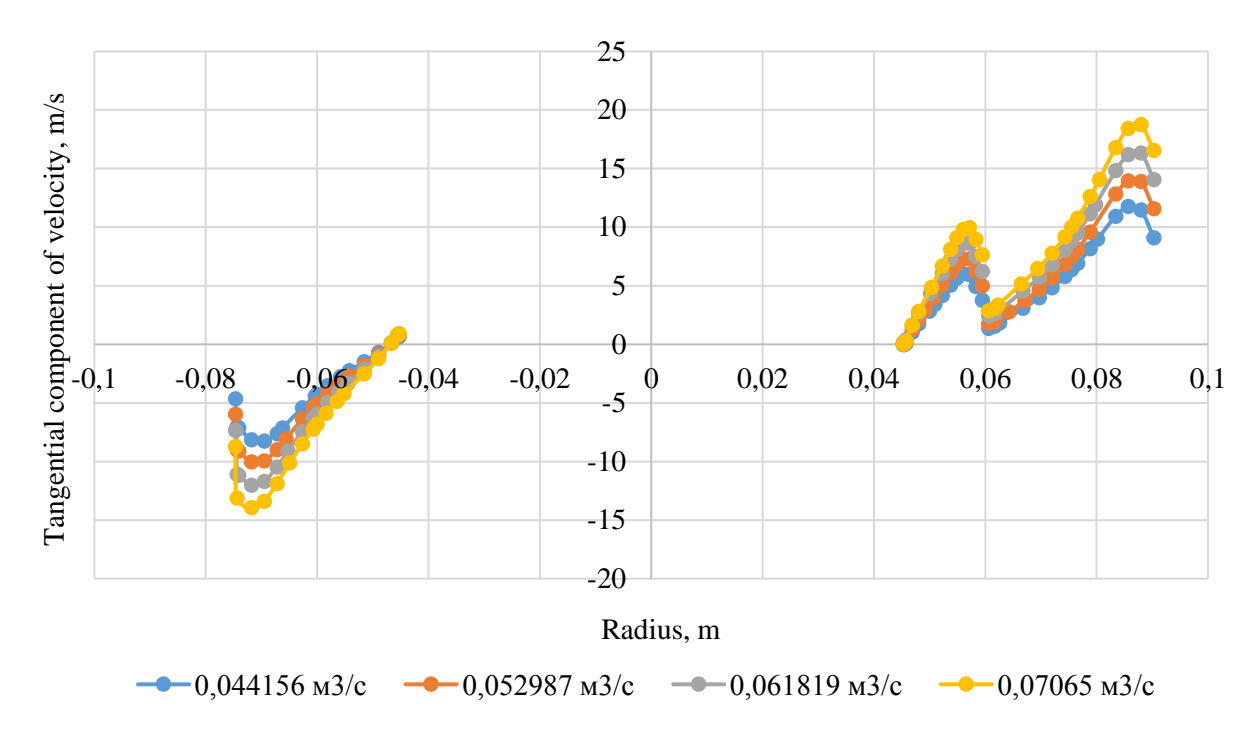


Fig. 8. Distribution of the tangential velocity component in the cross section of a spiral direct-flow cyclone operating on the suction line

For both operating modes (discharge and suction), the absolute value of the tangential velocity increases with increasing gas flow rate across the entire range of radii. This is expected, since a larger volumetric gas flow leads to higher speeds of movement and intensification of the vortex flow within the limited volume of the cyclone. The increase in tangential velocity directly affects the value of the centrifugal force, which is critical for the efficiency of dust collection.

The general shape of the tangential velocity profile (growth from the center, reaching a maximum, and further decrease to the walls) changes according to the parabolic law [19] and is similar for both cases, which indicates the universality of the mechanism of vortex flow formation in this type of cyclones.

However, in Fig. 7 (discharge line), the velocity peaks are more pronounced and sharper, which indicates a more concentrated vortex motion. The drop in velocity near the walls also seems less abrupt, which may indicate a smaller influence of wall friction relative to the intensity of the flow itself.

Higher tangential velocities, observed when operating on the discharge line, should theoretically lead to more efficient dust collection, since centrifugal forces, which are proportional to the square of the tangential velocity, will be much greater. This will allow for more efficient separation of even small particles.

Comparative analysis of the distribution of the axial component of the velocity. The efficiency of dust collection in cyclones is largely determined not only by the tangential, but also by the axial component of the flow velocity. The axial velocity forms a spiral movement of the gas downwards to the dust outlet and an upward flow to the cleaned gas outlet. Understanding the axial velocity distribution in different operating modes of the cyclone (on the discharge and suction lines) is key to optimizing its design, minimizing secondary dust removal, and increasing the overall cleaning efficiency

Positive values of axial velocity correspond to downward flow, negative values to upward (reverse) flow. Both graphs (Fig. 9, 10) show the axial velocity distribution characteristic of cyclones. In the peripheral

part of the cyclone (for positive and negative radii remote from the center), a downward flow (positive values of axial velocity) is observed, which corresponds to the main movement of the contaminated gas to the conical part of the cyclone and the dust hopper. In the central part of the cyclone, a zone of reverse (upward) flow (negative values of axial velocity) appears, along which the purified gas rises to the outlet pipe. This structure is key for effective separation, as it ensures the separation of the purified gas from the main mass of dust.

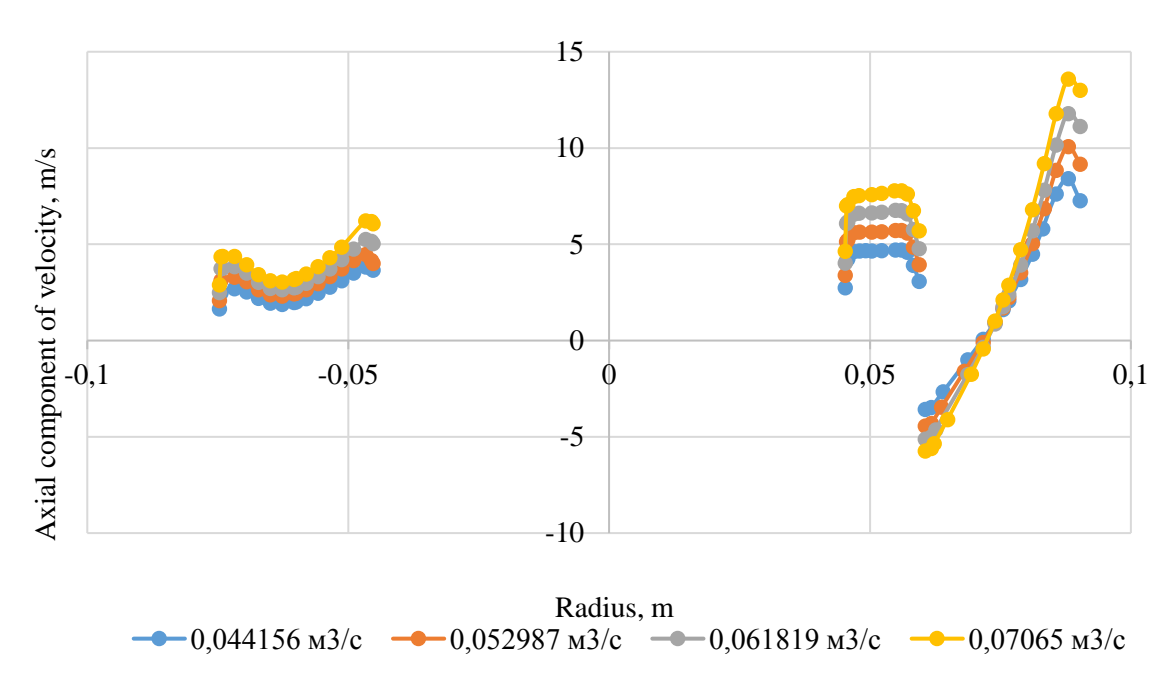


Fig. 9. Distribution of the axial velocity component in the cross section of a spiral direct-flow cyclone operating on the discharge line

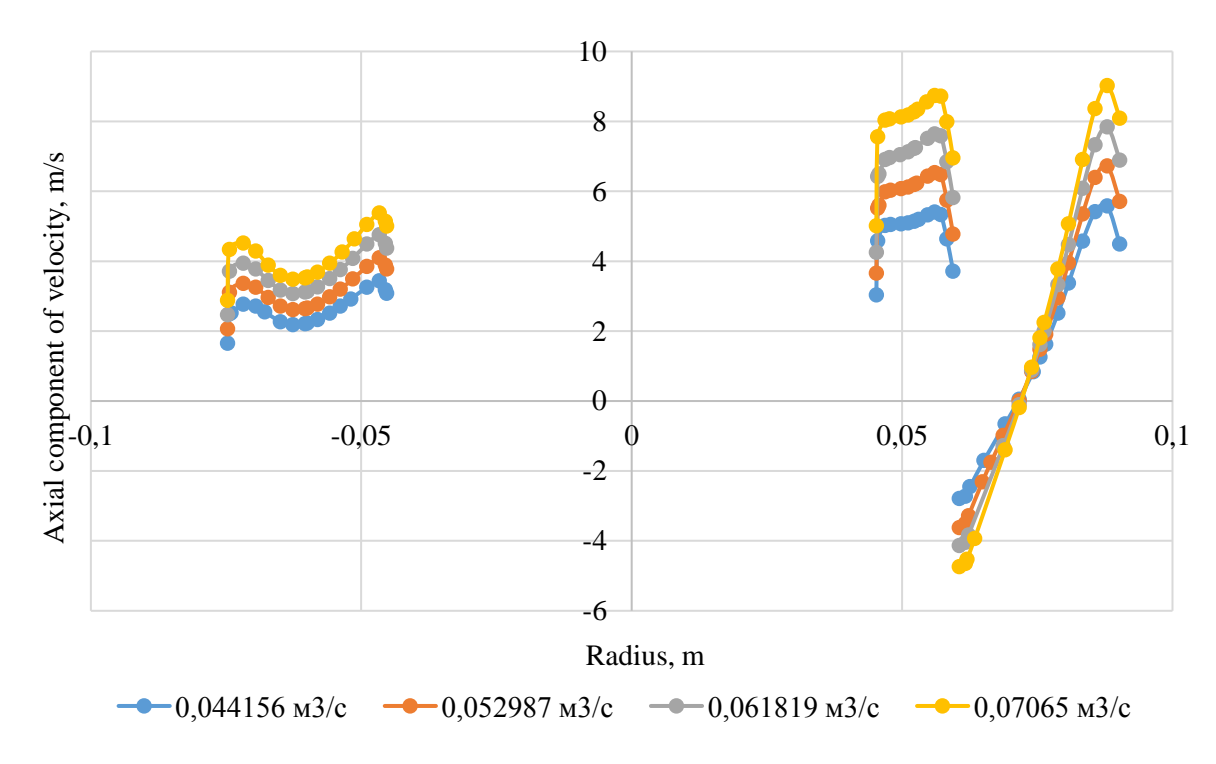


Fig. 10. Distribution of the axial velocity component in the cross section of a spiral direct-flow cyclone operating on the suction line

For both operating modes (discharge and suction), the absolute values of the axial velocity of both downward and upward flows increase with increasing gas flow rate. This is expected, since a larger volumetric gas flow leads to higher speeds within the limited volume of the cyclone. The increase in speeds indicates the intensification of aerodynamic processes.

On the discharge line (Fig. 9), the maximum positive values of the axial velocity (downward flow) reach about 13 m/s at the maximum flow rate. The maximum absolute negative values (upward flow) reach about -6 m/s. On the suction line (Fig. 10), the maximum positive values of the axial velocity (downward flow) reach about 9 m/s at the maximum flow rate. The maximum absolute negative values (upward flow) reach about -5 m/s.

Although reverse flow is observed in both cases, in Fig. 9 (discharge) its maximum absolute values are somewhat higher than in Fig. 10 (suction). A more intense reverse flow can both contribute to better removal of the cleaned gas and potentially increase the secondary removal of fine dust particles if the velocity exceeds the critical one for deposition.

The axial velocity distribution profile (increasing positive values at the periphery, crossing through zero, and the appearance of negative values in the center) is similar for both operating modes. This indicates a similar hydrodynamic flow formation mechanism. The transition point from downward to upward flow (zero axial velocity) is located at approximately the same radius for the corresponding flows in both cases.

Comparative analysis of the distribution of the radial velocity component. The radial velocity component plays a crucial role in the particle separation process in cyclones, as it determines the speed at which particles move from the center to the periphery of the device under the influence of centrifugal forces. Analysis of the radial velocity distribution enables us to estimate the intensity of particle deposition and understand how the aerodynamic conditions within the cyclone change depending on its location in the system, specifically on the discharge line or the suction line.

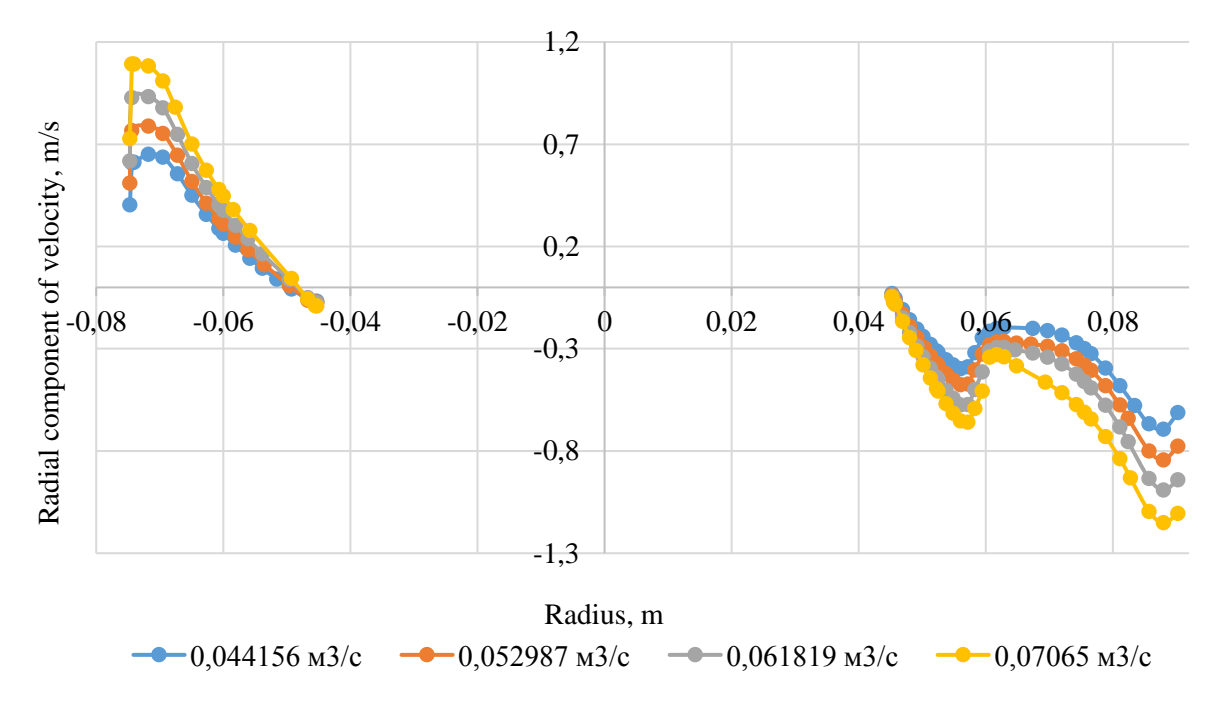


Fig. 11. Distribution of the radial velocity component in the cross section of a spiral direct-flow cyclone operating on the discharge line

Positive values of radial velocity correspond to flow movement from the center to the periphery, while negative values correspond to movement toward the center. In both graphs (Fig. 9, 10), a complex, yet characteristic, distribution of radial velocity for vortex devices is observed. In the near-wall region (large absolute values of radius, both positive and negative), a positive radial velocity is observed, indicating the

movement of gas from the center to the periphery. This is the result of the action of centrifugal forces, which throw the gas to the walls of the cyclone, contributing to the deposition of particles. In the central region (close to zero radius) negative values of radial velocity are observed, indicating the movement of gas to the center. This is due to the formation of a vortex core and reverse flows.

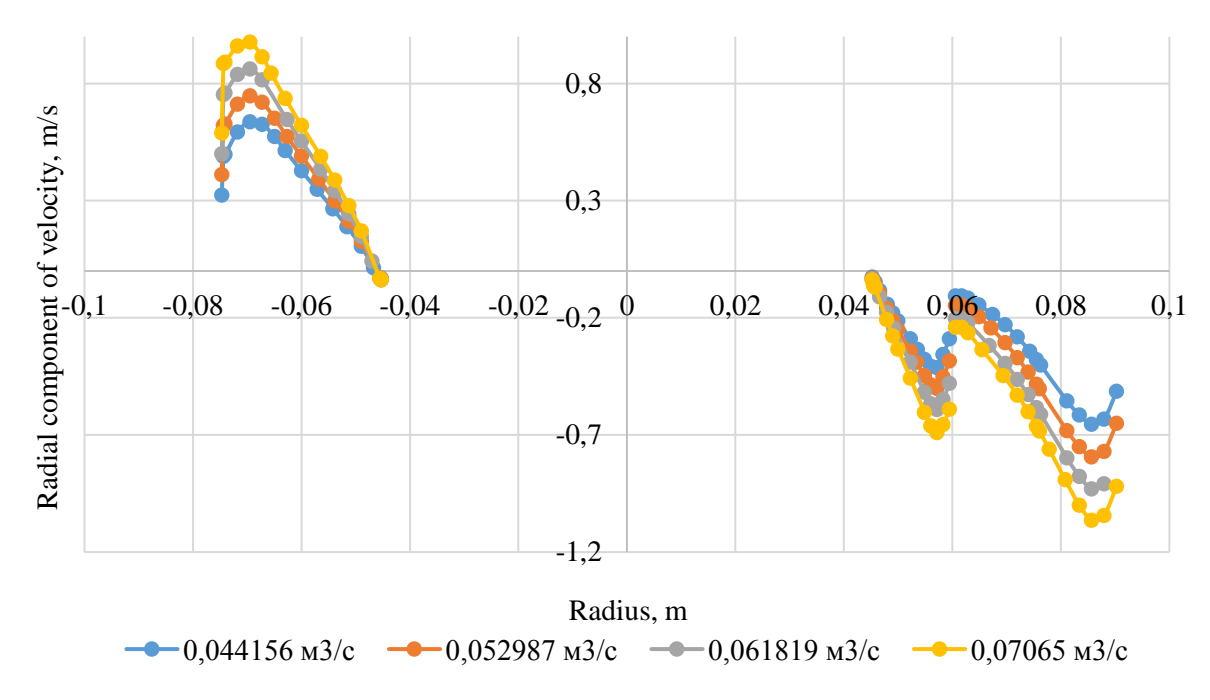


Fig. 12. Distribution of the radial velocity component in the cross section of a spiral direct-flow cyclone operating on the suction line

For both operating modes (discharge and suction), the absolute value of the radial velocity increases with increasing gas flow rate in most areas. This indicates an intensification of the radial movement of the gas, which, other things being equal, should have a positive effect on dust collection efficiency due to the increase in centrifugal forces.

On the discharge line (Fig. 11), the maximum positive values of the radial velocity reach about $1.1\,\text{m/s}$. The maximum absolute negative values reach about $-1.2\,\text{m/s}$. On the suction line (Fig. 12): The maximum positive values of the radial velocity reach about $0.9\,\text{m/s}$. The maximum absolute negative values reach about $-1.1\,\text{m/s}$.

In general, the absolute values of the radial velocity during cyclone operation on the discharge line are somewhat higher compared to operation on the suction line. This correlates with the previous analysis of the tangential and axial velocities and can be explained by the effect of pressure on the gas density. The gas under excess pressure (in the discharge line) has a higher density, which can lead to more intense radial movements at the same volumetric flow rates.

The general shape of the radial velocity profile is similar for both operating modes, which confirms the similarity of the hydrodynamic processes responsible for the formation of radial flows. However, it can be noted that in Fig. 11 (discharge line), the gradients of the radial velocity change seem somewhat steeper, especially in areas where the velocity changes sign. This may indicate sharper transitions in the flow character and more intense "pushing" of particles to the walls.

The presence of negative radial velocity values in the central part of the cyclone is important. This movement of gas towards the center can lead to secondary removal of small particles that have already been deposited, but due to turbulence, can again enter the central flow. Although the absolute values of these backflows are somewhat higher in the discharge line, their presence in both cases emphasizes the importance of optimizing the cyclone design to minimize this effect.

Comparative analysis of aerodynamic drag. The graph (Fig. 13) presents the obtained dependences of the aerodynamic drag of the cyclone on the velocity in the inlet nozzle.

For both operating modes (discharge and suction), a regular increase in aerodynamic resistance is observed as the gas velocity in the inlet increases. This dependence is close to quadratic, which is characteristic of turbulent flows in devices of this type, where pressure losses are mainly due to local resistance and friction.

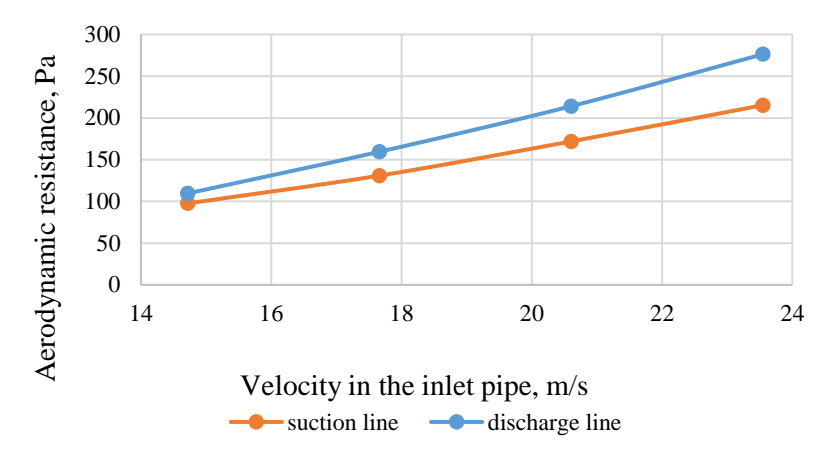


Fig. 13. Dependence of aerodynamic resistance on inlet velocity for a cyclone with a spiral cover

The key difference is that at any input velocity, the aerodynamic resistance of the device operating on the discharge line is higher than when operating on the suction line. At an inlet velocity of ~ 15 m/s, the difference is about 15 Pa. With an increase in velocity to ~ 23.5 m/s, this difference increases to more than 50 Pa.

This difference is probably explained by the nature of the flow entering the cyclone. When operating on the discharge line, a fan is installed in front of the cyclone, creating additional turbulence and unevenness in the velocity profile at the inlet to the device. This leads to more intense energy dissipation and, consequently, to greater pressure losses. On the contrary, when working on the suction line, the flow at the inlet is more laminar and stable, which provides less aerodynamic resistance.

Comparative analysis of cleaning efficiency. The graph (Fig. 14) illustrates the dependence of cleaning efficiency on the inlet velocity, assuming that particles are considered trapped if they reach the wall of the conical part of the device body.

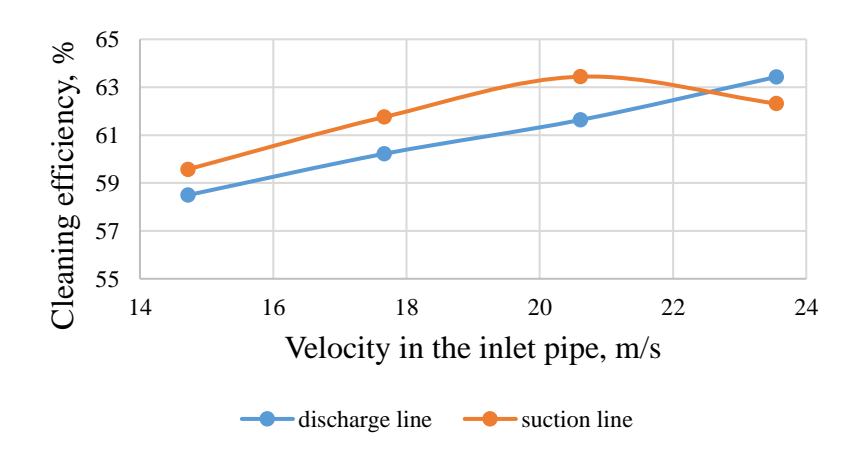


Fig. 14. Cleaning efficiency for the case where particles are considered captured if they reach the wall of the conical part of the device body

For this case, the device's operation on the suction line demonstrates higher efficiency in the speed range from 15 to ~23 m/s compared to its operation on the discharge line. When operating on the discharge

line, the cleaning efficiency increases almost linearly with increasing input speed throughout the studied range. When operating the device on the suction line, the efficiency increases until reaching a maximum value of approximately 63.4% at a speed of \sim 21 m/s, after which it begins to decrease. This may indicate the occurrence of the phenomenon of secondary capture (break-up) of already transferred dust particles to the wall of the device at too high flow speeds. The overall efficiency level for this case is relatively low, with a maximum of 64%. This is because the interaction of dust particles with each other is not taken into account. The graph (Fig. 15) shows the cyclone efficiency for the case when particles are considered captured when they reach the wall of the cylindrical part of the device body.

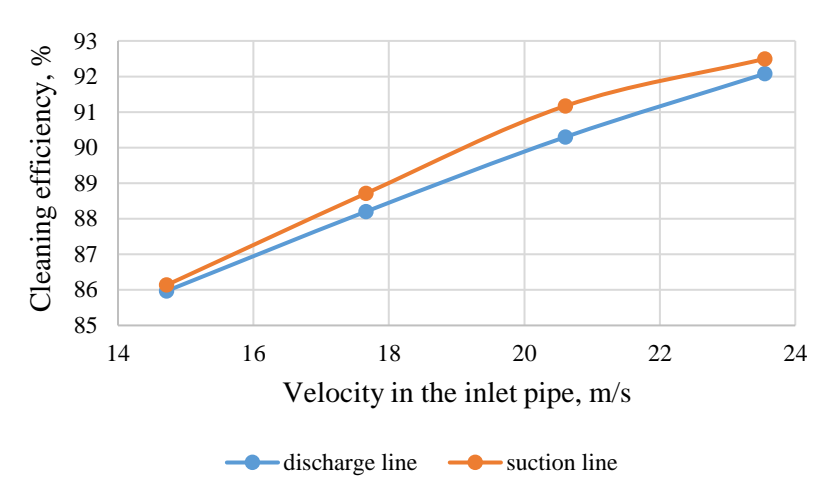


Fig. 15. Cleaning efficiency for the case where particles are considered trapped when they reach the wall of the cylindrical part of the apparatus body

As in the previous case, the operation on the suction line is more efficient than the operation on the discharge line in the entire range of inlet velocities. The difference in efficiency between the two modes increases slightly as the speed increases. For both modes of operation, a steady trend is observed, where the cleaning efficiency increases with increasing inlet velocity. Unlike the previous case, the effect of the decrease in cleaning efficiency at high velocities for the suction line is absent in the studied range.

To achieve maximum gas cleaning efficiency, this spiral direct-flow cyclone should be operated in the suction line operation mode. The optimal inlet velocity for such a configuration lies in the upper part of the studied range (21-24 m/s).

Comparative analysis of fractional cleaning efficiency. The fractional cleaning efficiency for the case where particles are considered to be trapped if they reach the wall of the cylindrical part of the device body is significantly higher in all ranges of particle diameters than the cleaning efficiency for the case where particles are considered to be trapped if they reach the wall of the conical part of the device body.

Figure 16 shows a graph of fractional efficiency for the device operating on the suction line with a gas flow rate of $0.07065 \text{ m}^3/\text{s}$. A similar picture is observed for all gas flows and operating modes of the device.

For particles with a size of 3–8 μ m, the difference in fractional efficiency is most noticeable. For example, for particles with a diameter of 5 μ m, the capture efficiency for the case when particles are considered captured if they reach the wall of the conical part of the device body is about 17 %, while for the case when particles are considered captured when they reach the wall of the cylindrical part of the device body, the efficiency reaches almost 85 %. For large particles (over 10 μ m), the difference in fractional efficiency decreases. For particles with a diameter of 20 μ m, the capture efficiency for the case where particles are considered captured if they reach the wall of the conical part of the device body reaches almost 100 %, which practically coincides with the efficiency for the case where particles are considered captured when they reach the wall of the cylindrical part of the device body. This indicates that large particles (larger than 10 μ m) have sufficient inertia to be effectively separated, and the influence of secondary flows on them is insignificant. The capture efficiency of particles with a size of 3–8 μ m depends on the magnitude of the secondary flows and the probability of collisions between particles.

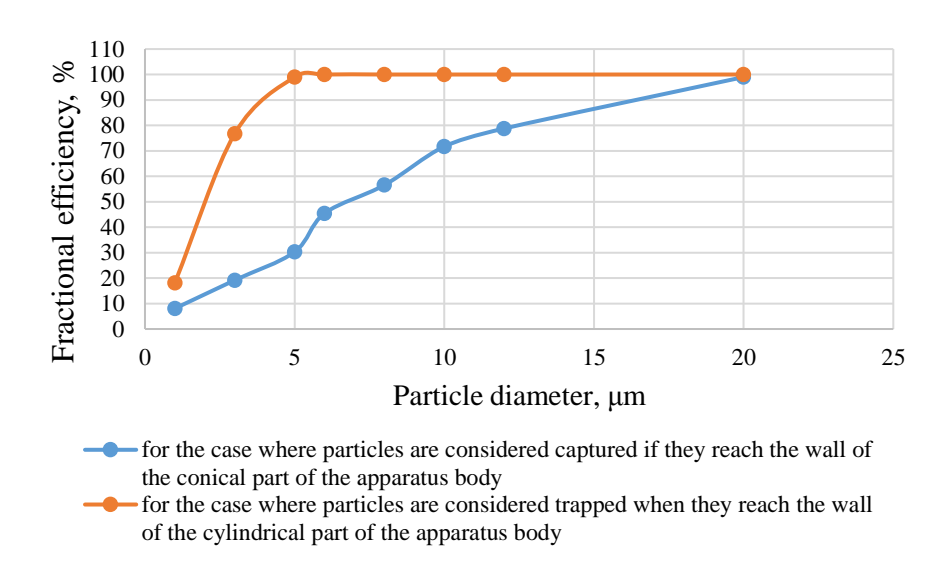


Fig. 16. Fractional efficiency of particle capture in the device

Conclusions

Having analyzed the gas flow motion, aerodynamic resistance, and cleaning efficiency in a spiral direct-flow cyclone during operation on the discharge and suction lines, the following conclusions can be drawn:

- 1. A comparative analysis of the velocity distribution in a spiral direct-flow cyclone demonstrates that the basic aerodynamic patterns (formation of a vortex flow with maximum velocities in the middle part and their decrease towards the center and walls) are preserved regardless of whether the cyclone operates on the discharge line or on the suction line; the absolute values of the velocities are higher when the cyclone operates on the discharge line, which is probably due to the higher gas density under excess pressure; an increase in gas flow leads to a proportional increase in velocities throughout the cyclone volume, which indicates an intensification of the vortex motion.
- 2. Analysis of the tangential velocity distribution in a spiral direct-flow cyclone shows that the main regularities of the formation of a tangential vortex flow, which are decisive for the operation of the cyclone, are its growth from the center to a certain distance and subsequent fall to the walls; an increase in gas flow leads to a significant increase in tangential velocities in both operating modes, which directly proportionally increases the intensity of centrifugal forces; the absolute values of the tangential velocity are significantly higher when the cyclone operates on the discharge line. This provides more intense vortex motion and, potentially, higher dust collection efficiency.
- 3. Comparative analysis of the axial velocity distribution in a spiral direct-flow cyclone demonstrates that the fundamental regularities of the formation of downward and upward flows are preserved both when the cyclone operates on the discharge line and on the suction line; an increase in gas flow rate leads to an intensification of both downward and upward flows, which is manifested in an increase in their absolute values; axial velocities in a cyclone operating on the discharge line are, as a rule, higher compared to a cyclone on the suction line; understanding these differences is important for the design and operation of cyclones, in particular for predicting the efficiency of particle capture and the risks of secondary dust removal.
- 4. Analysis of the radial velocity distribution in a spiral direct-flow cyclone confirms that the regularities of radial flow formation are preserved both when the cyclone operates on the discharge line and on the suction line; an increase in gas flow rate leads to an increase in radial movements, which potentially improves the separation efficiency; absolute values of radial velocity are generally higher when the cyclone operates on the discharge line, which indicates a more intensive deposition of particles under these conditions due to the effect of pressure on gas density; the presence of reverse radial flow zones in the central region is a critical aspect that must be considered when designing cyclones to minimize secondary dust removal.

- 5. The aerodynamic drag of the cyclone is directly proportional to the inlet flow velocity, and from an energy efficiency point of view, operating the cyclone on the suction line is more appropriate, as this provides lower pressure losses in the system.
- 6. Fractional efficiency analysis shows that secondary flows and particle interaction have a great influence on the efficiency of fine dust capture.

References

- [1] F. Qian, J. Lu, & Q. Guo, Numerical simulation of gas-solid flow in a cyclone separator using k–ε turbulence model. *Powder Technology*, 174(1–3), 23–31. 2007. doi.org/1016/j.powtec.2006.12.011.
- [2] A. C. Hoffmann, & L. E. Stein, *Cyclones: Design, Operation, and Maintenance*. CRC Press. 2008. doi.org/ 10.1007/978-3-540-77433-3.
- [3] M. D. Slack, & R. M. Davies, CFD simulation of turbulent flow in a cyclone separator using different turbulence models. *Chemical Engineering Science*, 73, 166–175. 2012. doi.org/10.1016/j.ces.2012.02.001
- [4] K. W. hu, & J. J. Ma, LES simulation of gas-particle flow in a cyclone separator. *Powder Technology*, 264, 258–267. 2014. doi.org/10.1016/j.powtec.2014.05.044.
- [5] J. Gimbun, T. G. Chuah, T. S. Y. Choong, & A. Fakhru'l-Razi, CFD simulation of cyclone separator performance with different cone angles. *Journal of Hazardous Materials*, 125(1–3), 140–147. 2005. doi.org/10.1016/j.jhazmat.2005.05.023.
- [6] R. Jiao, Y. Li, B. Wang, & J. Qian, Numerical simulation of gas-solid flow in a novel tangential-inlet cyclone with varying geometric parameters. *Separation and Purification Technology*, 157, 1–11. 2016. doi.org/10.1016/j.seppur.2015.11.025.
- [7] K. Elsayed, & M. Lacor, Discrete phase model for predicting the performance of a cyclone separator. *Powder Technology*, 203(2), 220–230. 2010. doi.org/10.1016/j.powtec.2010.05.016.
- [8] Y. Zhao, Q. Li, T. Li, & X. Wu. CFD-DEM simulation of gas-solid flow in a cyclone separator with consideration of particle-particle interaction. *Powder Technology*, 329, 16–27. 2018. doi.org/10.1016/j.powtec. 2018.01.036.
- [9] L. Wang, J. Liu, & X. Cai. Numerical simulation of flow field in a multi-cyclone separator. *Chemical Engineering Science*, 64(2), 488–494. 2009. doi.org/10.1016/j.ces.2008.09.021.
- [10] A. Safi, & A. Ahmadpour. CFD modeling and optimization of an axial-flow cyclone separator. *Separation Science and Technology*, 52(14), 2261–2270. 2017 doi.org/10.1080/01496395.2017.1336181.
- [11] J. H. Kim, Y. K. Lee, & J. D. Kim, CFD analysis and experimental investigation of pressure drop in a cyclone separator. *Journal of Industrial and Engineering Chemistry*, 12(4), 589–595. 2006.
- [12] W. Peng, Y. Li, J. Qian, & W. Wu, Numerical investigation on the separation performance of cyclone with consideration of particle shape and density. *Powder Technology*, *355*, 41–52. 2019. doi.org/10.1016/j.powtec.2019.06.059
- [13] Y. Su, C. Ma, C. Li, & H. Wang, Multi-objective optimization of cyclone separator based on CFD simulation and genetic algorithm. *Chemical Engineering Science*, 211, 115286. 2020. doi.org/10.1016/j.ces.2019.115286.
- [14] C. Zhu, L. Huang, & H. Hu, CFD simulation and experimental study of particle erosion in a cyclone separator. *Wear*, 478–479, 203875. 2021. doi.org/10.1016/j.wear.2021.203875.
- [15] L. Chen, S. Xu, & R. Li, CFD simulation of electrostatic enhancement of particle separation in a cyclone separator. *Journal of Electrostatics*, *118*, 103759. 2022. doi.org/10.1016/j.elstat.2022.103759.
 - [16] S. V. Patankar, Numerical heat transfer and fluid flow, Hemisphere, Washington, 1980.
- [17] A. I. Dubynin, V. V. Maistruk, R. I. Gavriliv, Tsyklony iz spiral'nym napravlyayuchym aparatom. [Cyclones with a spiral guide device]. Skhidno–Yevropeys'kyy zhurnal peredovykh tekhnolohiy [East–European Journal of Advanced Technologies]. Kharkiv, 2011 issue 2/6(50). pp. 35–37.
- [18] V. V. Maistruk, Optimization of cyclone operating modes with intermediate dust removal using gas flow structure analysis. *Ukrainian Journal of Mechanical Engineering and Materials Science*, vol. 8, No. 1, 2022, https://doi.org/10.23939/ujmems2022.01.020.